ART & TECHNOLOGY PUBLISHING PTE. LTD.

Information Engineering and Applied Computing

2022 Volume 1, Issue 1

ISSN: 2630-4619

Development of Path Tracking Algorithm and Variable Look-Ahead Distance Algorithm to Improve the Path-Following Performance of Autonomous Tracked Platform for Agriculture

Kyuho Lee[1], Bongsang Kim[1], Hyohyuk Choi[1], Heechang Moon[2]*

[1]Autonomous Vehicle & Intelligent Robotics Program, Hongik University, Seoul, Republic of Korea

[2]Mechanical and System Design Engineering Department, Hongik University, Seoul, Republic of Korea

***Corresponding author:** Heechang Moon, hcmoon@hongik.ac.kr

Abstract

With the advent of the 4th industrial revolution, autonomous driving technology is being commercialized in various industries. However, research on autonomous driving so far has focused on wheel-type platforms. Research on a tracked platform is at a relatively inadequate step. Since the tracked platform has a different driving and steering method from the wheel-type platform, the existing research cannot be applied as it is. Therefore, a path-tracking algorithm suitable for a tracked platform is required. In this paper, we studied a path-tracking algorithm for a tracked platform based on a GPS sensor. The existing pure pursuit algorithm was applied in consideration of the characteristics of the tracked platform. To compensate for the "cutting corner", which is a disadvantage of the existing pure pursuit algorithm, an algorithm that changes the LAD according to the curvature of the path was developed. In the existing pure pursuit algorithm that used a tracked platform to drive a path including a right-angle turn, the RMS path error in the straight section was 0.1034 m and the RMS error in the turning section was measured to be 0.2787 m. On the other hand, in the variable LAD algorithm, the RMS path error in the straight section was 0.0987 m, and the RMS path error in the turning section was measured to be 0.1396 m. In the turning section, the RMS path error was reduced by 48.8971%. The validity of the algorithm was verified by measuring the path error by tracking the path using a tracked robot platform.

Keywords

Tracked vehicle
Agricultural robot
Path tracking

1. Introduction

As the Fourth Industrial Revolution is sweeping across the globe, various technologies such as Artificial Intelligence (AI), robotics, Internet of Things (IoT), and autonomous driving are rapidly advancing. Among these, autonomous driving technology is making significant progress, driven by the decreasing costs of various sensors. This has led to research and development of autonomous driving using robots or vehicles in various industries. In particular, the agriculture sector is experiencing a rapid aging of its workforce, leading to a decrease in labor availability. To address this labor shortage, various research efforts are underway in the field of autonomous driving [1]. Currently research in the agricultural sector can be broadly categorized into the robotics field and the agricultural machinery field.

In the robotics field, technologies such as laser range finder (LRF) sensors [2], cameras [3], and Light Detection and Ranging (LiDAR [4]) sensors have been utilized to develop autonomous weeding robots for rice farming. Additionally, agricultural robots that can follow users on an infinite track have been developed [5-7], utilizing global positioning systems (GPS), LiDAR, and cameras for navigation. In the agricultural machinery field, research has focused on combines and tractors. Studies related to steering control for combine harvesters have been conducted, including path-following using simulators [8,9]. In Japan, research has been conducted on path planning and following for autonomous combines [10]. Tractors, being similar to automobiles, have also been the subject of various research projects concerning path-following [11-13].

Real-world validation of autonomous driving using actual tractors has been performed in Korea and overseas. Furthermore, in the agricultural field, vehicles often operate on uneven terrain such as unpaved roads, rugged terrain, or open fields. Consequently, the operating environment is challenging, with factors such as friction between the ground and the platform, the irregular shape of the unstructured terrain, and ground collapse during operation. Therefore, tracked platforms with a wide contact area with the ground have been preferred over wheeled platforms. However, previous research in autonomous driving has largely focused on Ackermann steering platforms and has been centered around automotive applications. Consequently, research on low-speed operation has been relatively limited. Thus, there is a need for the development of path-following algorithms suitable for agricultural platforms.

This study proposes an algorithm that adjusts the forward-looking distance according to the curvature of the path to enhance path-following performance at low speeds. The goal is to minimize path errors while accurately following the path.

2. Kinematic model of tracked platform

2.1. Kinematic model of tracked platform

To consider the geometry of a tracked platform, it is assumed that the platform is positioned on the horizontal plane (X_0, Y_0, Z_0) of the inertial coordinate system. The reference coordinate axes (X_P, Y_P, Z_P) of the platform are defined with respect to the platform's center of gravity (COG). The COG in the inertial coordinate system is represented by (x, y, z). Vertical motion due to vibrations generated while the platform is in motion is neglected, so only horizontal motion on the (X_P, Y_P) plane is considered, and the movement along Z_P axis is not taken into account [14].

The velocity of the tracked platform, as Z_P axis is not considered, can be represented as movement in the horizontal plane (X_P, Y_P) or v_y, v_y, denoted as $\vec{v} = [v_x, v_y, 0]^T$. Since there is no changes in coordinate for angular velocities, they are represented as $\vec{w} = [0,0,w]^T$. Assuming the COG vector of the platform is $\vec{p} = [x, y, \theta]^T$, the velocity vector can be expressed as $\vec{v} = [\dot{x}, \dot{y}, \dot{\theta}]^T$. The variables $\dot{x}, \dot{y}$ are related to the velocity vector of the platform, and rotational motion on the horizontal plane is $\theta = \omega$.

2.2. Skid steering

Skid steering is a steering method used by tracked platforms where the difference in speed between the inner and outer tracks is used to facilitate turning when the platform pivots. The steering radius of the platform is defined using the speed ratio between the inner and outer tracks and the turning radius of each track, as expressed by the following equations. However, this study does not consider the lateral slip that occurs between each track and the ground [15].

Figure 1 shows the free-body diagram of a tracked platform, and **Figure 2** represents the factors that influence the turning radius of a tracked platform.

$$v_o : v_i = R + \frac{B}{2} : R - \frac{B}{2} \quad (1)$$

$$\frac{v_i}{v_o} = \frac{R-\frac{B}{2}}{R+\frac{B}{2}} = i \quad (2)$$

$$R = \frac{B(1+i)}{2(1-i)} \quad (3)$$

Here, v_0 is the velocity of the outer track of a tracked platform, v_i is the velocity of the inner track of a tracked platform, R is the turning radius of a tracked platform, B is the width of a tracked platform, and i is the velocity ratio of a tracked platform.

3. Path following algorithm for tracked platforms

3.1. Overview

Path-following is defined as the process in which an autonomous driving platform follows a given path by executing appropriate steering actions. Precise path-following is essential, intending to minimize lateral distance errors between the platform and the path while approximating the platform's direction of movement to that of the path to ensure driving stability.

3.2. Pure pursuit

Pure pursuit is one of the representative methods for path following, along with the Stanley controller. It involves drawing a circular arc with two points, the current center coordinates of the platform and the target reference point. The algorithm calculates the diameter of this arc to determine the steering angle of the platform. **Figure 3** provides a brief illustration of path-following for a tracked platform.

The distance from the center coordinates of the platform to the target reference point is defined as the

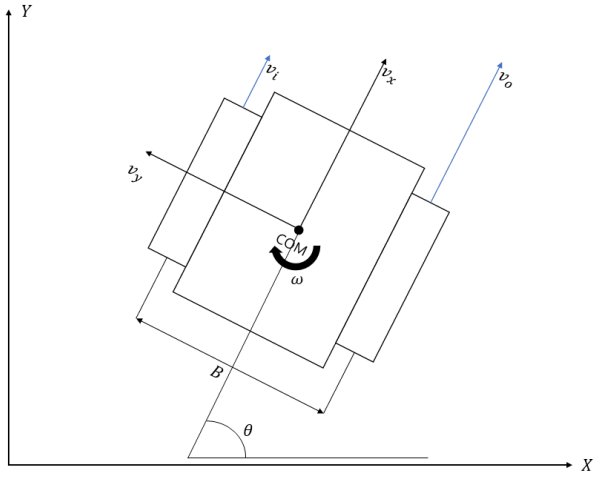

Figure 1. The free-body diagram of a tracked platform

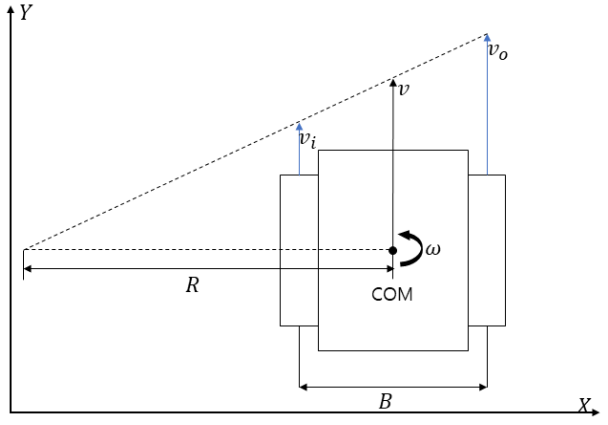

Figure 2. Factors of turning radius of tracked platform

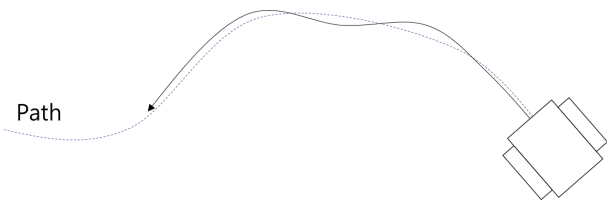

Figure 3. Path tracking of the autonomous tracked platform

look-ahead distance. When the look-ahead distance changes, the diameter of the circular arc drawn from the center of the platform also changes, leading to different steering angles being calculated for the platform. In pure pursuit, if the look-ahead distance is short, path-following performance improves, but there may be oscillations as the steering angle changes frequently while the platform follows the path. On the other hand, if the look-ahead distance is long, path-following performance may decrease, but the stability of the platform's motion improves as the steering angle changes less frequently. Therefore, setting an appropriate look-ahead distance is a crucial variable for achieving stable path-following[16,17]. **Figure 4** provides a simplified depiction of the platform's behavior based on the look-ahead distance.

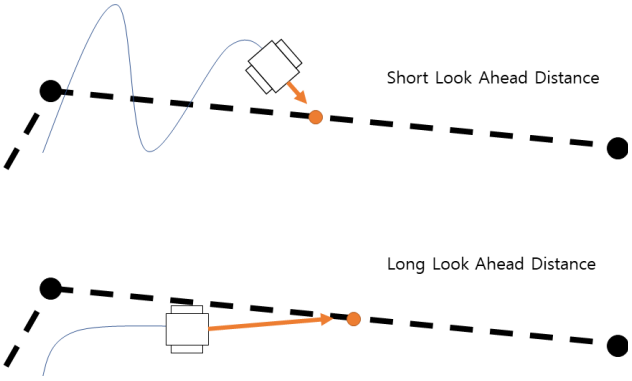

Figure 4. Comparison of look-ahead distance

In the existing pure pursuit method, the steering angle is calculated using the curvature of a circular arc with two points: the center position of the rear wheel and the target reference point of the platform, based on a bicycle model. However, for a tracked platform, where there are no limits to the steering angle and wheelbase, modifications are necessary. Considering the characteristics of a tracked platform, a geometric model shown in **Figure 5** can be drawn using the center coordinates (x_p, y_p) of the platform and the target reference points (x_L, y_L) determined by the look-ahead distance. By employing this geometric model, the following relationship can be obtained, which can be used to calculate the steering angle of the platform.

$$\tan\alpha = \frac{X}{Y} \tag{4}$$

$$\alpha = \tan^{-1}\left(\frac{X}{Y}\right) \tag{5}$$

$$\theta = -\delta - \alpha \tag{6}$$

Here, X is the x-axis distance from the current center coordinates of the tracked platform to the target reference point, Y is the y-axis distance from the current center coordinates of the tracked platform to the target reference point, θ is the steering angle of the tracked platform, and δ is the current direction of motion of the tracked platform.

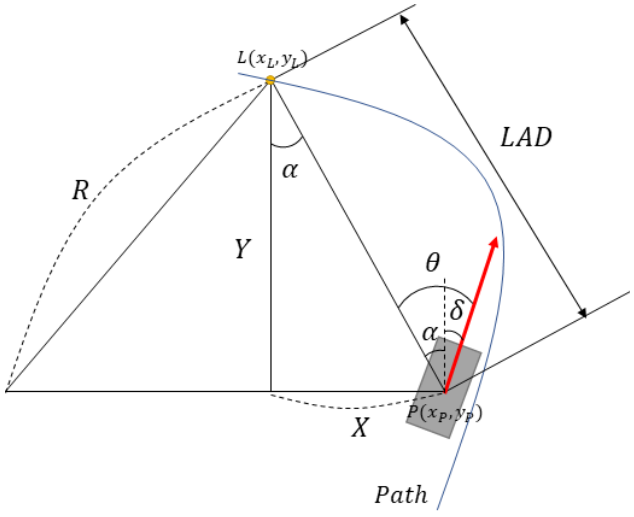

Figure 5. Pure pursuit geometric model of the tracked platform

3.3. Steering control algorithm

The pure pursuit algorithm was implemented in this study taking into consideration the characteristics of skid steering for tracked platforms. Using the steering angle calculated through pure pursuit, the speed ratio of the tracked platform was calculated. By substituting the turning radius with the speed and angular velocity using the correlation equation (3), it can be simplified into equation (7). When rearranging equation (7) for the steering ratio i, the equation (8) was obtained. **Figure 6** illustrates the sequence of steering values being output.

$$\frac{v}{\dot{\theta}} = \frac{B(1+i)}{2(1-i)} \quad (7)$$

$$i = \frac{2v-B\dot{\theta}}{2v+B\dot{\theta}} \quad (8)$$

Here, v is the current platform velocity, $\dot{\theta}$ is the target steering angular velocity, B is the width of the platform, and i is the steering ratio.

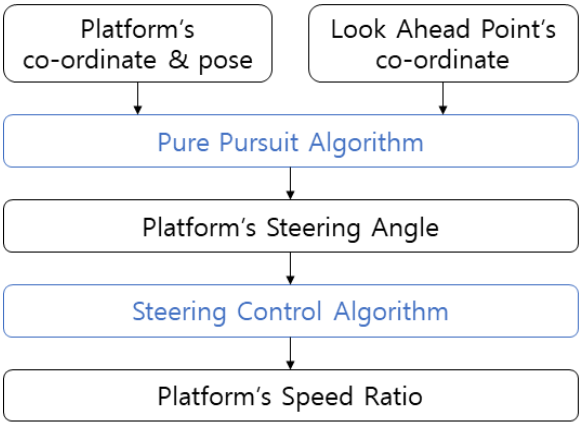

Figure 6. Steering command output flowchart

3.4. Path-following algorithm validation experiment

3.4.1. Experiment location and platform

This experiment was conducted at the Hwaseong Campus of Hongik University. For the experiment, a tracked platform was used. **Figure 7** shows a photograph of the tracked platform used in this experiment, and the specifications of the tracked platform are provided in **Table 1**.

Figure 7. Tracked platform used in the experiment

Table 1. A specification table of tracked platform

Size	H × L × W = 600 × 1,150 × 900 mm
Weight	90 kg
Drive speed	Max. 5 kph
Driving mode	Remote control & autonomous driving
Drive source	Electric battery, Li-ion 25.2 V / 80 Ah, 2,000 Wh * 1 EA (full charging 29.5 V)

Table 2. A specification table of ZED-F9P

Accuracy of the time pulse signal	Root mean square (RMS)	30 ns
	99%	60 ns
Frequency of time pulse signal	0.25 Hz to 10 MHz	
Velocity accuracy	0.05 m/s	
Dynamic heading accuracy	0.3 deg	
Operational limits	Dynamic	≤ 4 g
	Altitude	80,000 m
	Velocity	500 m/s
Horizontal pos accuracy	PVT	1.5 m CEP
	RTK	0.01 m
Vertical pos accuracy	RTK	0.01 m

3.4.2. Experimental methods and results

In this path-following experiment, the look-ahead distance was set as a variable, and experiments were conducted to observe the platform's behavior at each look-ahead distance increment of 1 meter. The driving speed was set at 3 kph, as this speed is typical for agricultural operations where the average working speed is generally within 3 kph. For position estimation in this experiment, the U-Blox ZED-F9P GPS sensor was used, and its specifications are detailed in **Table 2**. To obtain accurate platform position data, the VRS-GPS method was utilized to reduce GPS errors to a level of 1 cm, thus ensuring precise platform position data.

3.4.3. Conclusion of the path-following experiment

When the look-ahead distance is short, the target reference point is closer, resulting in a smaller curvature, allowing the platform to enter the path quickly. However, excessive changes in the steering angle, as seen in **Figure 8**, can lead to lateral control divergence and oscillations. Conversely, when the look-ahead distance is long, the curvature between the platform and the target reference point is larger, resulting in smoother path-following with fewer changes in the steering angle. Nonetheless, in situations where the actual platform has not yet entered the corner but the target reference point is already at the corner, it may lead to the "cutting corner" behavior, where the platform turns inwards more than necessary. This phenomenon becomes more pronounced as the look-ahead distance increases, as observed in the path-following experiment results from **Figures 8–12**.

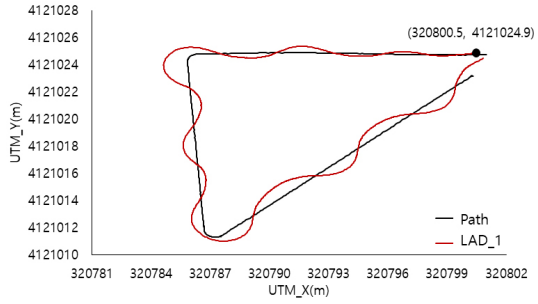

Figure 8. The trajectory of the platform according to the LAD 1 m

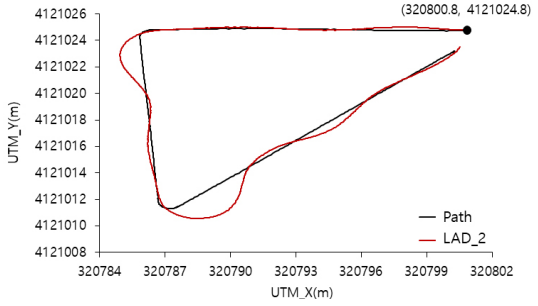

Figure 9. The trajectory of the platform according to the LAD 2 m

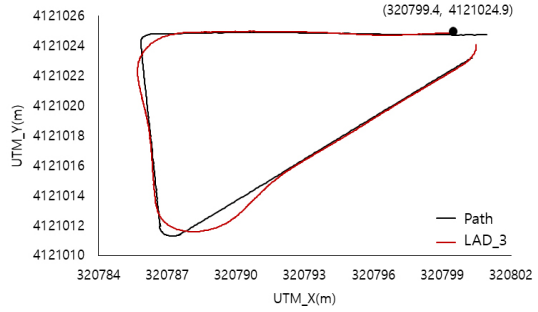

Figure 10. The trajectory of the platform according to the LAD 3 m

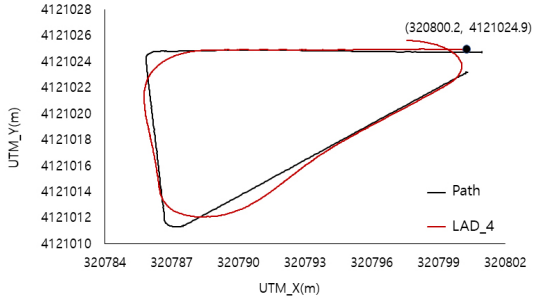

Figure 11. The trajectory of the platform according to the LAD 4 m

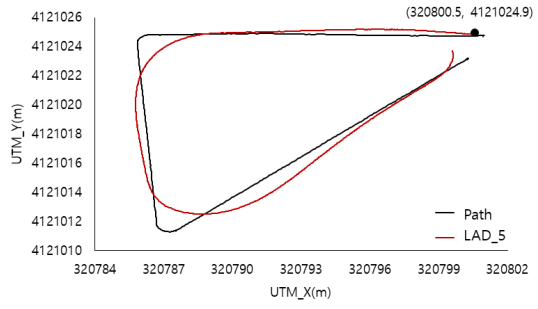

Figure 12. The trajectory of the platform according to the LAD 5 m

4. Variable look-ahead distance algorithm for path-following enhancement

4.1. Overview

When the look-ahead distance remains constant, various error phenomena occur in path-following depending on the look-ahead distance. When the look-ahead distance is short, there are rapid changes in the steering angle, leading to the "oscillation" phenomenon. On the other hand, when the look-ahead distance is long, especially in corner sections, the platform has not yet entered the corner, but the target reference point is already at the corner, resulting in the "cutting corner" phenomenon, where the platform turns inward more than necessary compared to the actual path. To reduce such path-following errors, autonomous vehicles often improve control performance by adjusting the look-ahead distance according to the vehicle's speed. However, in the case of agricultural tracked platforms, which operate at low speeds, changes in the look-ahead distance based on speed have limited impact. To address this, an algorithm that adjusts the look-ahead distance according to the curvature of the path followed by the platform was proposed.

4.2. Look-ahead distance for curvature calculation

To calculate curvature, it is necessary to determine the location at which curvature on the path should be computed. In the case of autonomous vehicles that travel at high speeds, the look-ahead distance for calculating curvature is adjusted in real-time based on speed, but in the case of autonomous agricultural operations, which operate at low speeds, there is no need to dynamically change the look-ahead distance for curvature calculation in real-time. Nevertheless, the look-ahead distance for curvature calculation should be greater than or equal to the look-ahead distance used for path following. This is because if the look-ahead distance for curvature calculation is smaller than the look-ahead distance for path following, it can lead to situations where the platform calculates the curvature of a straight path even though it is already following a curved path. In such situations, the platform's behavior may become unstable. In this study, through experiments with an existing path-following algorithm, a default look-ahead distance of 3 meters was selected as it minimizes the occurrence of "oscillation" and "cutting corner" phenomena when the platform is following a path.

4.3. Calculation and assessment of curvature on the path

The curvature was calculated using the coordinates of the target reference point on the path and the coordinates of the nearest point on the path obtained through GPS at the current platform position. To calculate the curvature, the unit vectors of the target reference point and the nearest point on the path were obtained. The coordinates of the target reference point and the waypoint immediately following the target reference point were used to obtain the unit vectors. Similarly, the unit vector at the nearest point was calculated using the same method as for the target reference point's unit vector.

$$P_n = \left(x_{P_n}, y_{P_n}\right), L_n = \left(x_{L_n}, y_{L_n}\right) \tag{9}$$

$$\widehat{x_{P_n}} = \frac{x_{P_{n+1}} - x_{P_n}}{\left(x_{P_{n+1}} - x_{P_n}\right)^2 + \left(y_{P_{n+1}} - y_{P_n}\right)^2} \tag{10}$$

$$\widehat{y_{P_n}} = \frac{y_{P_{n+1}} - y_{P_n}}{\left(x_{P_{n+1}} - x_{P_n}\right)^2 + \left(y_{P_{n+1}} - y_{P_n}\right)^2} \tag{11}$$

$$\widehat{x_{L_n}} = \frac{x_{L_{n+1}} - x_{L_n}}{\left(x_{L_{n+1}} - x_{L_n}\right)^2 + \left(y_{L_{n+1}} - y_{L_n}\right)^2} \tag{12}$$

$$\widehat{y_{L_n}} = \frac{y_{L_{n+1}} - y_{L_n}}{\left(x_{L_{n+1}} - x_{L_n}\right)^2 + \left(y_{L_{n+1}} - y_{L_n}\right)^2} \tag{13}$$

Here, P_n is the coordinates of the nearest point on the path for the tracked platform, and L_n is the coordinates of the target reference point. After obtaining the components of the two unit vectors, the

angle between the two unit vectors was calculated:

$$\theta = \cos^{-1}\frac{(\widehat{P_n}\cdot\widehat{L_n})}{(\|\widehat{P_n}\|\cdot\|\widehat{L_n}\|)} \quad (14)$$

The curvature of the path was then calculated using the sine law for the angle between the two vectors:

$$\kappa = \frac{\sin\frac{\theta}{2}}{\frac{|\overline{P_nL_n}|}{2}} \quad (15)$$

Based on the calculated curvature, it was determined whether the path being followed was a straight path or a curved path, and the look-ahead distance for path-following was decided accordingly. **Figure 13** shows the flow of curvature calculation.

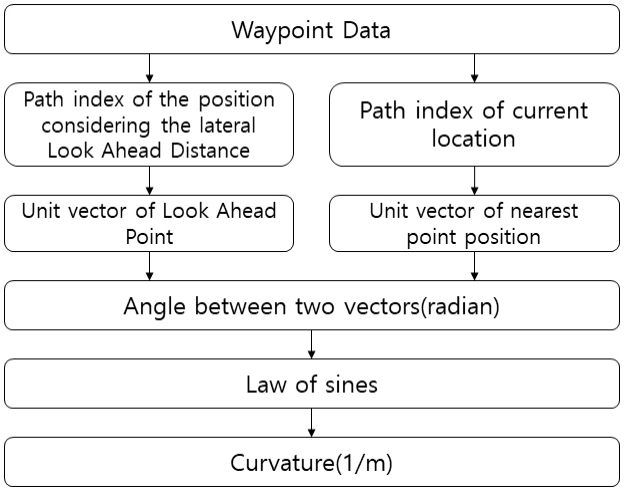

Figure 13. Curvature calculation flowchart

4.4. Path error

The metric used to assess path-following performance is the path error, defined as the length *D* of the line perpendicular to the path being followed from the current platform position. The actual path consists of point elements known as waypoints. To accurately measure the path error, the waypoints were interpolated as straight lines. The points used for linear interpolation were the *n*-th and *n*+1-th waypoints, considering the platform and the nearest point on the path as references. The path error was then calculated using the formula for the distance between a point and a line. GPS errors were not considered. **Figure 14** illustrates the path error.

$$D = \frac{|(y_{n+1}-y_n)x_p+(x_n-x_{n+1})y_p+x_{n+1}y_n-x_ny_{n+1}|}{\sqrt{(y_{n+1}-y_n)^2+(x_n-x_{n+1})^2}} \quad (16)$$

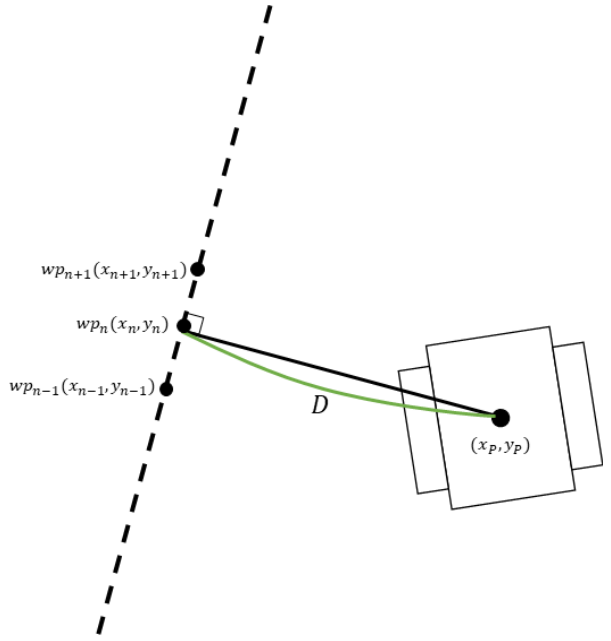

Figure 14. Definition of path error

4.5. Verification experiment of the variable look-ahead distance algorithm

4.5.1. Experiment location and platform

This experiment was conducted in the same place as the path following algorithm validation experiment at Hongik University's Hwaseong Campus, and the platform used was the tracked platform shown in **Figure 7**.

4.5.2. Experiment methods and results

In this driving experiment, both the existing fixed look-ahead distance algorithm and the developed variable look-ahead distance algorithm were tested. The same GPS sensor used in the path-following algorithm validation experiment was employed in this experiment as well. The driving was conducted at a speed of 3 kph along the same path. **Figure 15** depicts the trajectories of the path and the algorithms. The existing fixed look-ahead distance algorithm had a root mean square (RMS) path error of 0.1034 m on straight segments and 0.2787 m on turning segments. On the other hand, the variable

look-ahead distance algorithm had an RMS path error of 0.0987 m on straight segments and 0.1396 m on turning segments.

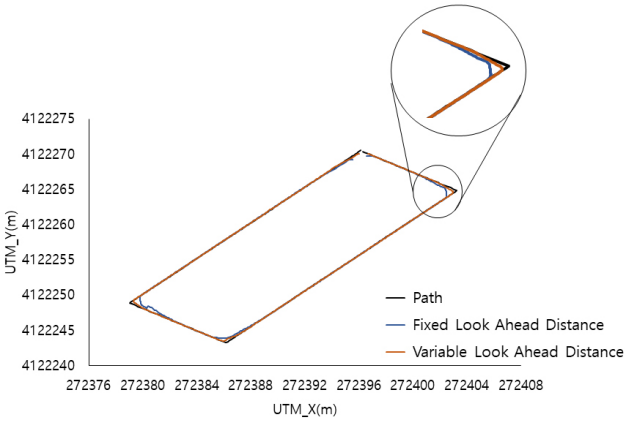

Figure 15. Experimental results of path-following algorithm and variable LAD algorithm

4.5.3. Experiment conclusion

The existing fixed look-ahead distance algorithm exhibited "cutting corners" behavior on right-angle turns, whereas it can be observed that the variable look-ahead distance algorithm approximates right-angle turns more closely. On straight segments, there is not much difference in path error, with only a 0.0047 m variation. However, on turning segments, there is a significant reduction in path error by approximately 48.9%, with a difference of 0.1931 m. The application of the variable look-ahead distance algorithm effectively reduced path error on turning segments.

5. Irregular environment driving experiment

5.1. Experiment overview

Driving experiments with variable paths were conducted, including right-angle turns and U-turns, in an irregular environment. In each path, the path error generated by the platform during its drive was measured to assess the path-following performance of the platform. The irregular environment was an open field in Goyang City, Gyeonggi Province, Korea, characterized by uneven terrain with weeds and soil, as shown in **Figure 16**. The GPS sensor in this experiment in an irregular environment was the same as in the previous experiments (**Figure 7**).

5.2. Driving on right-angle turning paths

Figure 17 shows the path followed by the tracked platform during the right-angle turn path and the trajectory it followed. As seen in **Figure 18**, the platform followed the path closely during straight segments, but path errors occur in right-angle turn segments compared to straight segments. The RMS path error during straight segments and right-angle segments was 0.1153 m and 0.1457 m, respectively. This represents an increase in RMS path error of 0.0304 m during the right-angle turn segments compared to straight segments.

Figure 16. Outfield in Goyang City, Gyeonggi Province, Korea

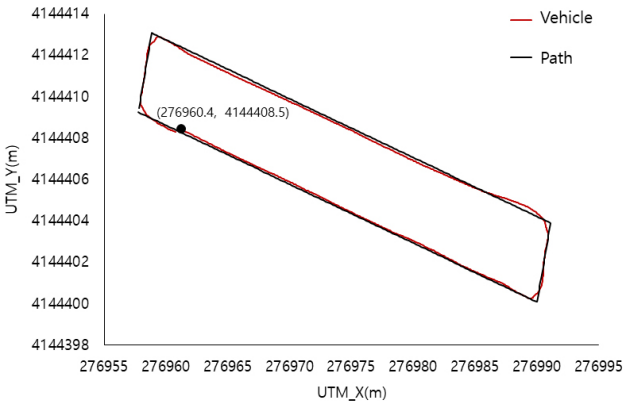

Figure 17. Right-angle turning driving in an irregular environment

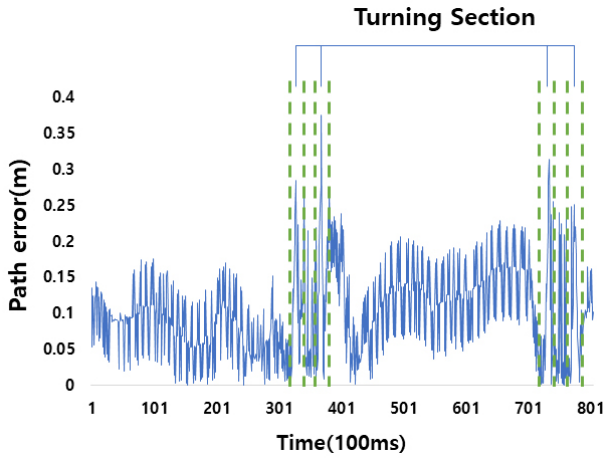

Figure 18. Right-angle turning driving error result in an irregular environment

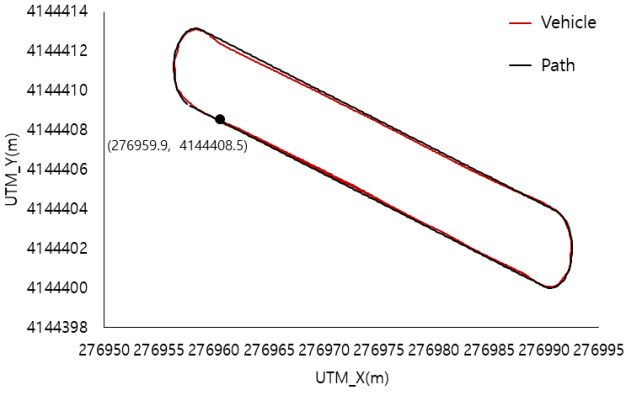

Figure 19. U-turn driving in an irregular environment

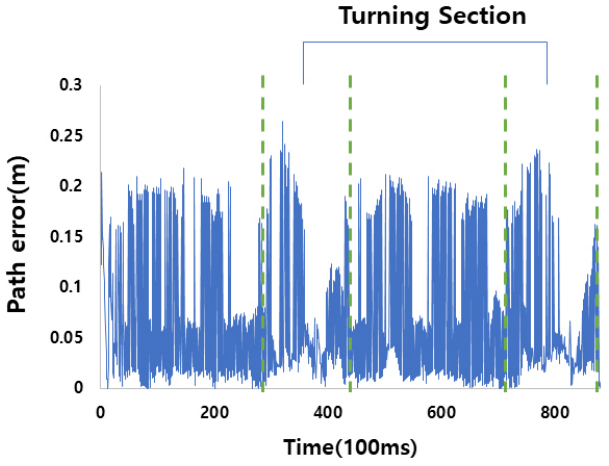

Figure 20. U-turn driving errors result in an irregular environment

5.3. U-turn paths

Figure 19 shows the path followed by the tracked platform during the U-turn maneuver in an irregular environment and the trajectory it followed. As seen in **Figure 20**, it is observed that the platform followed the path closely even during the U-turn segments, similar to the straight segments.

5.4. Analysis and discussion of driving experiments

5.4.1. Improving the "cutting corner" phenomenon

When driving with a fixed look-ahead distance of 3 meters, there is a phenomenon of turning inward from the path that occurs during right-angle turns. To compensate for this, an algorithm was developed to calculate the curvature of the driving path and change the look-ahead distance to 1 m when entering the turning section. This algorithm improved the "cutting corner" phenomenon and reduced path errors in right-turning segments by about 49%.

Nonetheless, the current variable look-ahead distance algorithm changes the look-ahead distance abruptly from 3 m to 1 m when the curvature increases. As a result, there may be instances where the look-ahead distance changes and the target heading point approaches rapidly, leading to a sharp increase in the steering angle. When the steering angle changes

abruptly, it can compromise the platform's driving stability, so further improvements are needed in the algorithm. In the future, an algorithm that gradually increases and decreases the look-ahead distance according to the curvature of the driving path will be developed to ensure driving safety.

5.4.2. Various path-following experiments

In this study, experiments on commonly standardized paths were conducted. Compared to wheeled platforms, the advantages of the tracked platform include the ability to pivot in place and the ability to drive on rough terrain. Thus, in the future, the platform's ability to follow paths with abrupt changes in steering angle, such as spiral paths and zigzag paths, in addition to right-angle and U-turn maneuvers, will be tested. Furthermore, experiments in various driving environments will be conducted to assess path-following performance on different terrains will be conducted.

5.4.3. Ensuring platform safety during driving

In this study, the tracked platform performed path following using only a GPS sensor. The experimental environment did not contain any obstacles, and it was a controlled setting, so relying solely on the GPS sensor posed no safety issues. Nevertheless, in real autonomous driving scenarios, platforms may encounter various obstacles and environments, necessitating the use of perception sensors. Perception sensors can detect obstacles and assist in decisions such as stopping or evasive maneuvers. Additionally, research should be conducted on algorithms that can serve as alternatives in case the GPS sensor experiences instability.

6. Conclusion

In this study, a path-following algorithm was developed based on the pure pursuit method, taking into account the characteristics of the tracked platform. Using this algorithm, path-following experiments were conducted, but the path errors increased in turning segments due to the "cutting corner" phenomenon, which is one of the characteristics of pure pursuit. To improve this issue, an algorithm that dynamically adjusts the look-ahead distance based on the curvature of the path was developed, which is a crucial variable in determining the steering angle in pure pursuit. Through experiments, it was confirmed that the variable look-ahead distance algorithm based on curvature significantly reduced path errors compared to the existing path-following algorithm.

Last but not least, for the tracked platform to achieve autonomous driving, additional research is planned to incorporate perception sensors such as LiDAR or cameras alongside GPS. These sensors will provide the platform with the ability to perceive its surroundings, allowing it to navigate even in cases where GPS sensor errors occur.

Disclosure statement

The authors declare no conflict of interest.

Funding

This work was funded by Ministry of Agriculture, Food and Rural Affairs (MAFRA), "Development of Eco-Friendly Small and Medium Sized Weeding Robots for Agricultural Assistance in Fields such as Soy" (Project Number: 321061-2) and supported by the publication grant.

References

[1] Kim BS, Cho SW, Moon HC, 2020, Slip Detection and Control Algorithm to Improve Path Tracking Performance of Four-Wheel Independently Actuated Farming Platform. Journal of Korea Robotics Society, 15(3): 221–232. https://doi.org/10.7746/jkros.2020.15.3.221

[2] Kim GH, Kim SC, Hong YK, et al., 2012, Detection of Rice Seeding and Path Planning for an Autonomous Weeding Robot in a Paddy Field. Proceedings of the KSAM and ARCs 2018 Autumn Conference, 17(1): 100–103. https://kiss.kstudy.com/Detail/Ar?key=3697182

[3] Kim GH, Kim SC, Hong YK, 2014, Method of Image Processing for Rice Seedlings Detection of Weeding Robot. Proceedings of the KSAM and ARCs 2014 Autumn Conference, 19(2): 85–86. https://kiss.kstudy.com/Detail/Ar?key=3273682

[4] Yang C, Won J-H, Hong Y, et al., 2021, Study on Caterpillar Type Weeding Robot Based on Environment Recognition Using LiDAR. Proceedings of the KSAM and ARCs 2021 Autumn Conference, 26(2): 226. https://kiss.kstudy.com/Detail/Ar?key=3911353

[5] Kim J-H, Kim M-J, Beak S-W, et al., 2018, Development of Leader-Follower Tracked Vehicle for Agriculture Convergence of Skid Steering and Pure Pursuit using β Compensation Coefficient. Journal of Institute of Control Robotics and Systems, 24(11): 1033–1042. https://doi.org/10.5302/J.ICROS.2018.18.0163

[6] Kim J-H, Kim HW, Lee JU, 2019, Using β coefficient for Convergence of Skid Steering and Pure Pursuit Development of Rotation Ability Compensation Algorithm for Leader-Follower Agricultural Tracked Vehicle. 2019 Korean Society of Automotive Engineers Fall Conference and Exhibition, 2019: 694–699. https://www.dbpia.co.kr/journal/articleDetail?nodeId= NODE09295642

[7] Kim J-H, Kim HW, Lee JU, 2020, Development of Navigation Algorithm Based on the Geometric Method for Self-Driving of the Tracked Vehicle: Convergence of Skid Steering and Pure Pursuit Using Compensation Coefficients. 2020 Korean Society of Automotive Engineers Fall Conference and Exhibition, 2020: 738–742. https://www.dbpia.co.kr/journal/ articleDetail?nodeId=NODE 10519447

[8] Jeon C-W, Kim H-J, Han X, et al., 2017, Preliminary Study on Automated Path Generation and Tracking Simulation for an Unmanned Combine Harvester. Proceedings of the KSAM and ARCs 2017 Autumn Conference, 22(1): 20. https://kiss.kstudy.com/Detail/Ar?key=3517454

[9] Jeon C-W, Kim H-J, Kim J-H, et al., 2017, Application of a Combine Harvester Driving Simulator for Autonomous Path Tracking and Steering Control. Proceedings of the KSAM and ARCs 2017 Autumn Conference, 22(2): 69. https://kiss.kstudy.com/Detail/Ar?key=3556078

[10] Kurita H, Lida M, Cho W, et al., Rice Autonomous Harvesting: Operation Framework. Journal of Field Robotics, 34(6): 1084–1099. https://doi.org/10.1002/rob.21705

[11] Han XZ, Kim HJ, Lee YT, et al., 2012, Study on Path Planning and Tracking Algorithms for an Auto-Guided Tillage Tractor. Proceedings of the KSAM and ARCs 2012 Autumn Conference, 17(1): 124–128. https://kiss.kstudy.com/Detail/Ar?key=3697188

[12] Han XZ, Kim HJ, Moon HC, et al., 2012, Research on Simulation of Path Tracking for Auto-Guided Tillage Tractor. Proceedings of the KSAM and ARCs 2012 Autumn Conference, 17(2): 36–40. https://kiss.kstudy.com/Detail/Ar?key=3862119

[13] Han DH, Byeon SJ, Kim KD, et al., 2021, Development of Path Tracking Control Algorithm for Tractor Autonomous Driving. Proceedings of the KSAM and ARCs 2021 Autumn Conference, 26(2): 107. https://kiss.kstudy.com/Detail/Ar?key=3911249

[14] Sidi MHA, Hudha K, Kadir ZA, et al. 2018 IEEE 14th International Colloquium on Signal Processing & Its Applications (CSPA), March 9–10, 2018: Modeling and Path Tracking Control of a Tracked Mobile Robot. 2018, Penang. https://doi.org/10.1109/CSPA.2018.8368688

[15] Han QJ, Liu SJ, 2013, Path Tracking Control of Tracked Vehicle. International Journal of Computer Science Issues, 10(6): 103–109. https://www.ijcsi.org/papers/IJCSI-10-6-1-103-109.pdf

[16] Coulter RC. Implementation of the Pure Pursuit Path Tracking Algorithm. 1992, The Robotics Institute, Carnegie-Mellon University.

[17] Snider JM. Automatic Steering Methods for Autonomous Automobile Path Tracking. 2009, The Robotics Institute, Carnegie-Mellon University.